Original Article
Early changes of NLRP3 inflammasome activation after hypoxic-ischemic brain injury in neonatal rats

Na Li[1,2], Chunying Liu[1], Chunnan Wang[2], Ruidan Chen[2], Xiaofeng Li[2], Yang Wang[2], Chunyu Wang[2]

[1]College of Integrated Traditional Chinese and Western Medicine, Liaoning University of Traditional Chinese Medicine, Shenyang, China; [2]Children's Neurorehabilitation Laboratory, Shenyang Children's Hospital, Shenyang, China

Abstract: The pathogenesis of neonatal hypoxic-ischemic (HI) brain injury may involve activation of the NOD-like receptor family pyrin domain-containing-3 (NLRP3) inflammasome and its downstream effectors, caspase-1 and interleukin (IL)-1β. The start time of therapy is associated with adverse neurodevelopmental outcome following HI injury. We performed this study investigating early dynamic changes in NLRP3, caspase-1, and IL-1β expression during the first 24 h following HI brain injury in an animal model, in order to optimize selection of treatment time after injury. Rats were randomized to an HI group (n=40) and sham group (n=40). Rats in the HI group were subjected to right common carotid artery ligation and then exposed to hypoxia (8% O_2) for 2 h, and divided into 5 subgroups with 8 cases in each group at 5 postoperative time points (0, 4, 8, 12, 24 h). Brain injury during the first 24 h after surgery/hypoxia was evaluated by cranial ultrasonography. RT-PCR, western blot, and immunohistochemistry were applied to determine protein and mRNA expressions. In the HI group, ultrasonography revealed accelerated right vertebrobasilar artery flow at 4 h, enhanced brain parenchyma echogenicity at 24 h, and blood stealing from the vertebrobasilar artery at 24 h. In the HI group, immunohistochemistry demonstrated elevated expressions of NLRP3 and IL-1β at 4, 8, 12, and 24 h and enhanced expression of caspase-1 at 8 and 12 h (all $P < 0.01$). Western blot and RT-PCR revealed that, compared with the sham group, the HI group exhibited elevated expression of NLRP3 at 4, 8, and 24 h, caspase-1 at 12 h, and IL-1β at 8 h (all $P < 0.05$). In summary, the present results suggested that activation of NLRP3/caspase-1/IL-1β signaling occurs within 4 h of HI brain injury in the neonatal rat.

Keywords: Neonatal hypoxic-ischemic brain injury, inflammasome NLRP3, caspase-1, interleukin-1β

Introduction

Hypoxic-ischemic encephalopathy (HIE) is a major cause of neonatal death and neurodevelopmental disorders [1]. About 18% of infants with moderate or severe HIE eventually die, and another 25% suffer from the sequelae of lifelong neurologic deficits such as cerebral palsy, mental retardation, epilepsy, visual and hearing impairment, learning and behavioral disorders, and attention deficit and hyperactivity disorder [2, 3]. Therapeutic hypothermia is the only clinically recognized method that can be used to treat HIE. The beneficial effects of moderate hypothermia is presumed to be a reduction of secondary energy failure which starts 6-8 hours after resuscitation [4]. However, nearly 31.6%-51.4% of infants with moderate or severe HIE who receive hypothermia still survived with disabilities [5-7]. It is still controversial as to when to start hypothermic treatment to achieve the best neuroprotective effect [8, 9]. The first six hours of life after hypoxic-ischemic (HI) episode is the window of opportunity to start hypothermic treatment, but in clinical practice exposure to HI is not clearly defined, and HI injury may have started before birth. Thus, the prevention and treatment of HI brain injury remain a great challenge. In current practice, the focus should be on finding ways to detect HIE as early as possible. This requires study of pathophysiologic changes of the brain in the early stage of hypoxic-ischemic brain injury, especially within 24 hours.

Inflammation is considered to be an important pathophysiologic factor of cerebral ischemic injury [10]. The NOD-like receptor family pyrin

domain-containing-3 (NLRP3) inflammasome is a multiprotein complex that can induce pyroptosis by the activation of caspase-1 and secretion of IL-1β and IL-18 [11]. Caspase-1 and NLRP3 have been implicated in a variety of nervous system diseases such as ischemic stroke, atherosclerotic plaque formation, Alzheimer's disease, Parkinson's disease, motor neuron disease, epilepsy, and glioma [12-15]. Notably, activation of NLRP3 signaling has also been detected following HI brain injury in neonatal rats [16-18], raising the possibility that the NLRP3 inflammasome, caspase-1, and IL-1β may be involved in the pathogenesis of neonatal hypoxic-ischemic (HI) brain damage. However, little is known about the time course of the changes in NLRP3, caspase-1, and IL-1β expression during the first 24 h after HI injury to the brain.

The aim of this study was to examine the dynamic changes in NLRP3, caspase-1, and IL-1β expression during the first 24 h following HI brain injury in an animal model. Our findings support a key role for NLRP3/caspase-1/IL-1β signaling in cerebral HI injury. This may provide a basis for timing of early treatment for HI brain injury.

Methods

Animals

Eighty 7-day-old neonatal Sprague Dawley rats weighing 10-14 g (Liaoning Changsheng Biotechnology Co. Ltd., Liaoning, China) were used in this study. All animals were maintained under specific pathogen-free conditions. For the experiments, the neonatal rats were randomly divided into an HI group (*n*=40) and a sham operation group (*n*=40). The HI models were established and divided into 5 subgroups with 8 cases in each group at 5 postoperative time points (0, 4, 8, 12, 24 h). All animals were euthanized at the end of the experiment. The study protocol was reviewed and approved by the Animal Ethics Committee of the Affiliated Hospital of Liaoning University of Traditional Chinese Medicine.

Animal model of HI brain injury

The *in vivo* HI model was induced by ligating the right common carotid artery as described previously [19, 20]. Each neonatal rat was anesthetized with 2-3% isoflurane and placed on the operating table in the supine position. The operation was carried out with the ambient temperature maintained at about 30°C. The neck skin was sterilized with 75% alcohol, and a 0.5-cm incision was made using ophthalmic scissors. The anterior cervical muscles and trachea were separated using ophthalmic forceps to expose the right common carotid artery. In the HI group, the right common carotid artery was double-ligated with no. 5 suture; ligation was not performed in the sham group. The skin was sutured, washed, and disinfected. After regaining consciousness, the rat was placed in a closed chamber at 37°C, and a hypoxic gas mixture comprising 8% O_2 and 92% N_2 was infused into the chamber at a velocity of 5 L/min. After 2 h, the rat was taken out of the chamber and returned to the mother's cage for raising. The overall adoption rate was 98%; 2 neonatal rats in the HI group were killed by the mother at 8 h and 12 h after being returned to the cage.

Neurological severity scoring

Another 8 suckling rats were subjected to ligation of the right common carotid artery and hypoxia for 2 h, then neurological severity scoring was performed at 4 h, 8 h, 12 h, 24 h, 48 h, 7 d, and 14 d after hypoxia-ischemia. Mice were scored as described previously according to Ludmila Belayev's 12 score system [21] by an individual blinded to experimental group. The system consisted of two tests that have been used previously to evaluate various aspects of neurologic function: (1) the postural reflex test was used to examine upper body posture while the animal is suspended by the tail. Scores are as follows: 0, no observable deficit; 1, limb flexion during hang test; 2, deficit on lateral push. And (2) the forelimb placing test was used to examine sensorimotor integration in forelimb placing responses to visual, tactile, and proprioceptive stimuli. Neurologic function was graded on a scale of 0 to 12 (normal score, 0; maximal score, 12).

Visual placing tests included forward and sideways stimuli. The experimenter held the animal in his hand, suspended its front paws in the air, and then placed it in front of the table and slowly leaned closer above the table from 10 centimeters. The normal response of the rat was to grab the table with the forelimb, and the response of the injured rats was delayed. Sideways stimulation meant that the animal

was located on the side of the table, and the experimental method was the same as the front stimulation. In the tactile placing tests, the eyes of the animal were covered, its front paws suspended in the air, and the dorsal surface of the paw was touched gently. The stimulation depth was only as deep as the skin and hair, and the animal's reaction and scores were the same as the visual placing tests. Similarly, we stimulated the lateral surface of paw slightly and repeated the above experiment. The proprioceptive placing test was the same as the tactile placing tests, but this test has only forward stimulation and the stimulation depth should reach the muscles and joints. The score was as follows: 0, complete placement immediately; 1, incomplete placement and/or delay (< 2 s); 2, vacancy.

Evaluation of success of the HI brain injury model by cranial ultrasonography

Two-dimensional ultrasonography (MyLab™ 30 Gold ultrasound system, Esaote, Genoa, Italy) using a fan-scan or linear array probe (6.6-12.0 MHz) was performed before and after surgery [22]. The head of the rat was fixed on the ultrasound workbench, and the probe was placed at the midline of the parietal bone. Sonographic images of the lateral ventricle and brain parenchyma were obtained to detect any lesions. The maximal end-systolic velocity (ESV), end-diastolic velocity (EDV), and resistance index (RI) of the proximal part of the bilateral middle cerebral artery (MCA) were measured. Brain injury was evaluated by acoustic radiative force pulse imaging (ARFI).

Histology and immunohistochemistry

Rats from each experimental group were sacrificed with 3%~4% isoflurane at 0 h, 4 h, 8 h, 12 h, or 24 h after surgery and then the brain tissue was collected and stored at -80°C before use. The brain tissue was fixed in 4% paraformaldehyde solution for 24 h, dehydrated in a graded series of alcohol, embedded in wax, and sectioned into 5 μm-thick slices. For histology, the paraffin sections were stained with hematoxylin-eosin (H&E) and observed by light microscopy. H&E staining was performed to evaluate the hypoxia-ischemia induced brain injury evaluation at 0 h, 4 h, 8 h, 12 h, 24 h.

For immunohistochemistry, the paraffin-embedded sections were routinely dewaxed, hydrated, and blocked with BSA for 30 min. The sections were then incubated overnight (12 h) at 4°C with the following primary antibodies: rabbit anti-NLRP3 polyclonal antibody (1:1000; ab214185, Abcam Cambridge, UK), rabbit anti-caspase-1 polyclonal antibody (1:500; YT5743, Immunoway Biotechnology, Plano, TX, USA) or rabbit anti-IL-1β polyclonal antibody (1:1000; ab205924, Abcam). After three washes in phosphate-buffered saline (PBS), the sections were incubated at 37°C for 30 min with horseradish peroxidase (HRP)-conjugated goat anti-rabbit monoclonal IgG (1:100; EPR4321, Abcam). After washing, the sections were stained using diaminobenzidine. The development of staining was observed under a microscope (TC-S-SR, Nikon, Tokyo, Japan), and the process of discoloration was terminated after 5-15 min by the addition of distilled water. The sections were then dehydrated and fixed using standard procedures, and images were acquired using fluorescence microscopy (Leica Microsystems Inc., Buffalo Grove, IL, USA). ImageJ software was used to analyze the expression of NLRP3, caspase-1, and IL-1β.

Western blot

Brain tissue samples were washed with ice-precooled PBS solution until bloodless, shredded, and homogenized. Cell lysate was prepared by ultrasonic homogenization in 1 mL ice-cold RIPA buffer (3 times for 10 s each with an interval of 30 s). The lysate was transferred to a 1.5-mL centrifuge tube and centrifuged at 4°C for 5 min at 12000 rpm. The supernatant was subjected to sodium dodecyl sulfate-polyacrylamide gel electrophoresis (40 μg total protein per lane), and a wet transfer to polyvinylidene difluoride membrane was carried out. After blocking for 1 h with 5% skim milk powder, the membrane was incubated overnight at 4°C with mouse anti-rat caspase-1 antibody (1:500), rabbit anti-rat NLRP3 polyclonal antibody (1:1000; ab214185; Abcam), or rabbit anti-rat IL-1β polyclonal antibody (1:1000; ab205924, Abcam). After washing, the membrane was incubated with HRP-conjugated goat anti-rat IgG (1:10000; EPR4321, Abcam) or HRP-conjugated goat anti-rabbit IgG (1:10000; ab205718, Abcam) for 1 h. The bands were visualized using the enhanced chemiluminescence technique. The relative expression level of the target protein was calculated as the ratio of the gray value of the target protein band to the gray value of the β-actin band (ab8226, Abcam).

Table 1. Primer sequences used for quantitative polymerase chain reaction

Primer	Sequence (5'-3')
NLRP3 upstream primer	5'-TGAAGAGTGTGATCTGCGGAAAC-3'
NLRP3 downstream primer	5'-GAAAGTCATGTGGCTGAAGCTGT-3'
Caspase-1 upstream primer	5'-GATGGACCTGACTGAAGC-3'
Caspase-1 downstream primer	5'-AGTGTAGGGACAATAAATGG-3'
IL-1β upstream primer	5'-GAGAGGGAAATCGTGCGT-3'
IL-1β downstream primer	5'-GGAGGAAGAGGATGCGG-3'

IL-1β: interleukin-1β; NLRP3: NOD-like receptor family pyrin domain-containing-3.

Real-time PCR

Total RNA was extracted with Trizol reagent (Ambion, Austin, TX, USA). Standard procedures to eliminate RNase were strictly followed. Glass and metal utensils were heated to 250°C for 4 h, and plastic utensils were soaked in diethyl pyrocarbonate (DEPC) solution for 24 h and then dried after high-pressure inactivation of DEPC. Reverse transcription of RNA to cDNA was performed using PrimeScript™ RT Master Mix (RR036A, Takara Bio, Shiga, Japan) according to the manufacturer's protocol. The primer sequences (**Table 1**) were synthesized by Shanghai Generay Biotech Co., Ltd. (Shanghai, China). PCR was carried out using the SYBR Premix Ex Taq™ II (Tli RNaseH Plus) real-time PCR kit (RR820, Takara) and a Heal Force CG-05 PCR instrument (Heal Force, Shanghai, China). The thermal cycle parameters were 95°C for 30 s, 95°C for 5 s and 60°C for 30 s for 40 cycles. The relative expression of mRNA was calculated using the $2^{-\Delta\Delta CT}$ method.

Statistical analysis

The analyses were performed using SPSS 17.0 (SPSS Inc., Chicago, IL, USA). The data were presented as the mean ± standard deviation (SD) and were compared between groups using the t-test for independent samples and variance analysis. Comparisons of data among multiple groups were performed using one-way analysis of variance (ANOVA) and the SNK post-hoc test. *P*-values < 0.05 were considered significant.

Results

General observations after exposure to hypoxia

Compared with animals in the sham operation group, rats in the HI group exhibited noticeably more head trembling and limb twitching during exposure to hypoxia in the chamber as well as paler skin and poorer peripheral circulation after 2 h of hypoxia. Although the above signs disappeared gradually with time, the activity level and duration of eye opening were lower for rats in the HI group than for animals in the sham operation group after their return to the mother's cage. Although two neonatal rats were killed by the mother during the experiment, there was no significant difference in adoption rate between the two groups.

Another 8 suckling rats were subjected to ligation of the right common carotid artery and hypoxia for 2 h, so that neurologic function can be assessed on a point scale of 0 to 12 (**Table 2**; **Figure 1**) at 4 h, 8 h, 12 h, 24 h, 48 h, 7 d, and 14 d after hypoxia-ischemia. In our study, the neurologic scores of postural reflex and placing test at 8 h were significantly higher than those at other time points (*P* < 0.05), and the symptoms of nerve injury gradually improved with the extension of resuscitation time.

Evaluation of the HI brain injury model by cranial ultrasonography

Cranial ultrasonography was used to evaluate the rats before surgery/exposure to hypoxia and at 0 h (i.e., immediately after), 4 h, 8 h, 12 h, and 24 h after surgery/exposure to hypoxia (**Figure 2**). In the HI group, the right vertebrobasilar artery had an accelerated blood flow velocity at 4 h after modeling, and parts of the brain parenchyma showed enhanced echogenicity at 24 h. Furthermore, three of the animals in the HI group exhibited the phenomenon of blood stealing from the vertebrobasilar artery at 24 h after modeling, and color Doppler flow imaging revealed that the blood flow in the vertebral artery was opposite to that in the ipsilateral common carotid artery. Pulsed Doppler imaging of the vertebral artery showed a reverse flow spectrum in both the systolic and diastolic phases.

Table 3 summarizes the data for EDV, ESV, and RI. When compared to the left MCA, the right MCA in the HI group had significantly lower ESV at 4 h and 24 h, lower EDV at 24 h and higher RI at 4 h, 12 h, and 24 h after surgery (all *P* < 0.05). Furthermore, the right MCA in the HI

Table 2. Neurological evaluation of rats with HI

Item	4 h	8 h	12 h	24 h	48 h	7 d	14 d	F value	P value
Postural reflex	1.75±0.00	1.98±0.46	1.38±0.74**	1.00±0.53***	1.00±0.53***	0.88±0.83**	0.63±0.91***	7.188	0.000
Visual placing	1.50±0.53	2.75±0.46	1.63±0.52	0.88±0.35***	0.88±0.35***	0.38±0.52***	0.25±0.46***	13.556	0.000
Tactile placing	1.75±0.46	2.25±0.46	2.00±0.00	0.88±0.64***	0.75±0.71***	0.38±0.74***	0.15±0.35***	19.327	0.000
Proprioceptive placing	1.75±0.46	1.88±0.64	1.63±0.74	1.00±0.53**	1.00±0.53**	0.38±0.74***	0.38±0.52***	8.556	0.000
Total score	6.75±0.89*	8.25±0.71	6.38±1.06**	3.75±1.16***	3.75±1.41***	2.00±1.41***	1.13±0.99***	45.006	0.000

Data are presented as mean ± standard deviation. Postural reflex scores are as follows: 0, no observable deficit; 1, limb flexion during hang test; 2, deficit on lateral push. Placing test scores are as follows: 0, complete immediate placing; 1, incomplete and/or delayed placing (< 2 s); 2, absence of placing. *$P < 0.05$, **$P < 0.01$, ***$P < 0.001$ vs. 8 h group.

group had significantly lower ESV and higher RI than the sham operation group at 24 h (all $P < 0.05$). The left MCA of the HI group exhibited a progressive increase in EDV and a temporary decrease in ESV at 4 h that was followed by a subsequent increase (**Table 3**). In the HI group, the RI of the left MCA at 4 h was significantly different from that at all other time points, and the RI of the right MCA at 4 h was significantly different from that at all other time points except 12 h (all $P < 0.05$; **Table 3**).

Histopathology of hippocampal and cerebral cortical brain tissue at various times after surgery/hypoxia

The structure of the right cerebral cortex was arranged neatly. The neurons were aligned and compact, and cell morphology was normal at 0 h. In the HI group, slight swelling, a few lipid droplets, partial nuclear fragmentation and interstitial homogenization were observed at 4 h. At 8 h, the cells swelled, lipid droplets decreased, and a small amount of red staining showed eosinophilic degeneration of neuronal cells. At 12 h, the eosinophilic changes of neuronal cells increased, showing nuclear pyknosis and mild cell body atrophy. At 24 h, the volume of neuronal fine cells, the number of cells, and the eosinophilic changes were decreased (**Figure 3A**).

In the HI group, histopathology of the pyramidal cell layer in the right hippocampus began to show red neurons and a decrease in cell density at 4 h. Cell density was further reduced and some cells had vacuole formation at 8 h. Volume and number of neuronal cells were reduced, and eosinophilic changes were decreased simultaneously at 12 h and 24 h (**Figure 3B**).

Expression of NLRP3, caspase-1, and IL-1β proteins in brain tissue evaluated by immuno-histochemistry

Representative images showing sections of brain tissue from the HI group stained using immunohistochemistry techniques are presented in **Figure 4A**. Compared with the expression level at 0 h, the expressions of NLRP3 and IL1-β were significantly elevated at 4 h, 8 h, 12 h, and 24 h ($P < 0.01$ for all), and the expression of caspase-1 was significantly enhanced at 8 h and 12 h ($P < 0.01$ for both; **Figure 4B**). Peak expression levels occurred at 8 h for NLRP3, 12 h for caspase-1, and 24 h for IL1-β (**Figure 4B**).

Expression of NLRP3, caspase-1 and IL-1β proteins in brain tissue evaluated by western blot

Figure 4A shows representative immunoblots illustrating the expression levels of NLRP3, caspase-1, and IL-1β proteins in brain tissue from the HI and sham operation groups at varying times after surgery/hypoxia. The general trends in the data over time indicated that, compared with the sham operation group, the HI group exhibited higher expression of NLRP3 from 4-24 h, and caspase-1 from 12-24 h and IL-1β from 8-24 h, although statistical significance was not attained at all time points (**Figure 5B**). Significant differences between groups were observed at 4 h, 8 h, and 24 h for NLRP3, 12 h for caspase-1, and 8 h for IL-1β ($P < 0.05$ for all; **Figure 5B**).

Expression of NLRP3, caspase-1, and IL-1β mRNA in brain tissue evaluated by RT-PCR

RT-PCR showed that changes in the expression patterns of NLRP3, caspase-1, and IL1-β mRNA over time in the two groups were broadly similar to the expression patterns of the correspond-
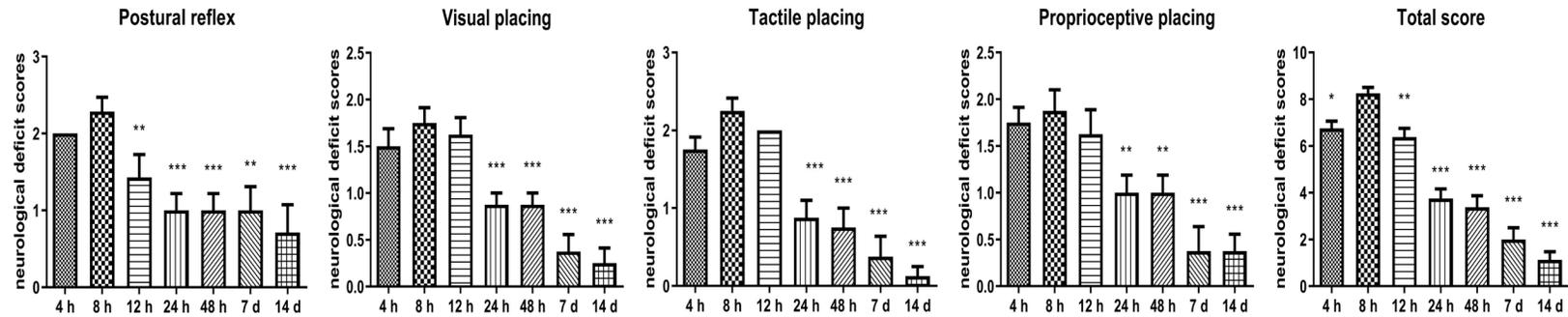
Figure 1. Neurological evaluation of rats with Ludmila Belayev 12 score system. *$P < 0.05$, **$P < 0.01$, ***$P < 0.001$ vs. 8 h group.
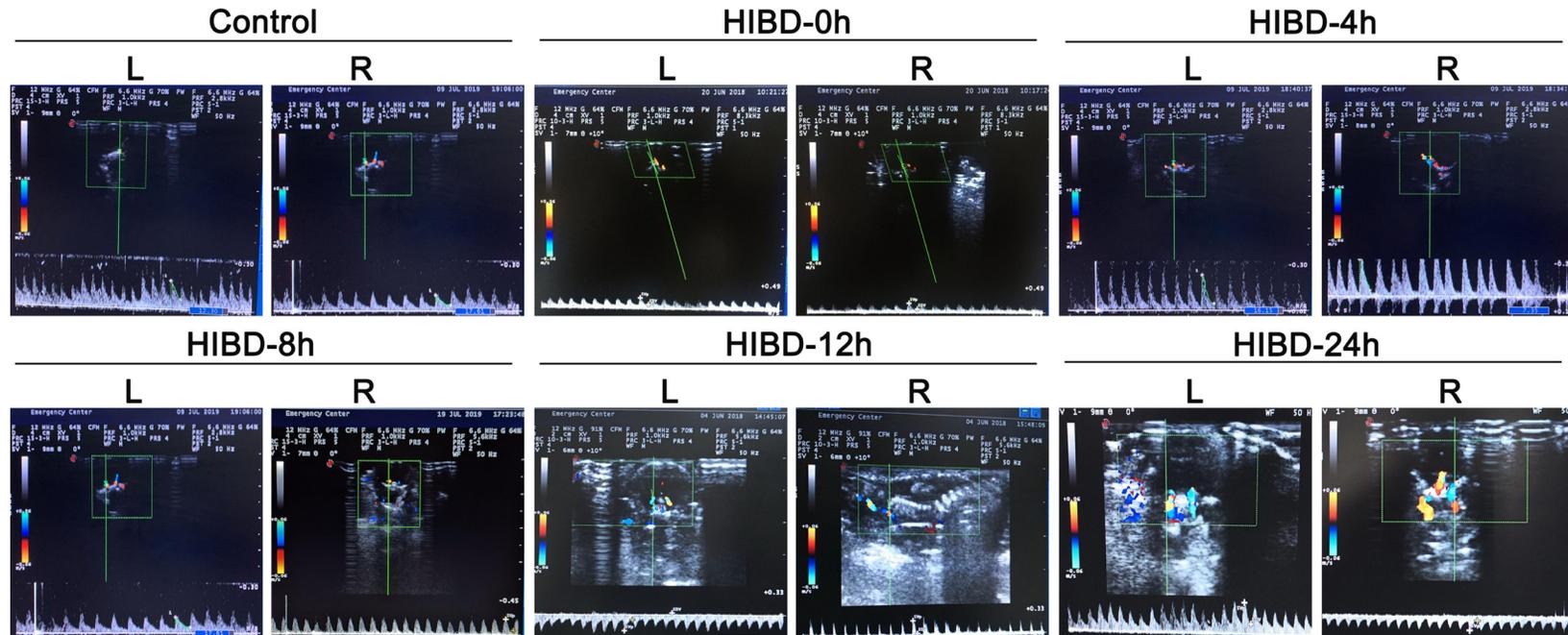
Figure 2. Evaluation of the HI brain injury model by cranial ultrasonography. Representative images are shown for the sham operation group at 24 h after surgery (Sham) and for the hypoxic-ischemic brain damage group at 0 h (i.e., immediately after surgery; HIBD-0 h), 4 h (HIBD-4 h), 8 h (HIBD-8 h), 12 h (HIBD-12 h) and 24 h (HIBD-24 h) after surgery. L: left side; R: right side. Blood flow velocity in the right vertebrobasilar artery was increased at 4 h after modeling. Parts of the brain parenchyma in the HIBD group showed enhanced echogenicity at 24 h. The right vertebral artery exhibited stenosis in its proximal segment. Blood flow through the left vertebral artery regurgitated through the basilar artery to the right side; this phenomenon of blood stealing was not observed in the other groups.

Table 3. End-diastolic velocity, end-systolic velocity, and resistance index measured by cranial Doppler ultrasonography

Group	Left middle cerebral artery			Right middle cerebral artery		
	EDV (cm/s)	ESV (cm/s)	RI	EDV (cm/s)	ESV (cm/s)	RI
Sham group at 24 h	26.80±1.00	9.20±0.30	0.60±0.02	23.20±4.30	11.60±0.40[*]	0.60±0.21
HI group 0 h	16.8±1.60[§]	6.50±0.40	0.60±0.02	17.00±1.10	5.90±0.30	0.60±0.01
HI group 4 h	19.1±5.50[§]	4.70±0.90[§]	0.70±0.08[§,a]	22.20±4.10	3.30±0.30[*,§]	0.80±0.03[*,§,a]
HI group 8 h	32.20±4.40[a,b]	13.40±1.50[a,b]	0.60±0.05[b]	24.60±6.90[a]	9.30±4.20[b]	0.60±0.05[b]
HI group 12 h	24.90±8.80	8.30±2.90[c]	0.70±0.04[b]	27.50±8.50	5.40±2.30	0.80±0.03[*,b,c]
HI group 24 h	40.50±2.60[a,b,d]	13.10±0.90[a,b,d]	0.70±0.03[b]	19.70±1.00[*]	4.00±0.80[*,§,b,c,d]	0.80±0.04[*,§,a,c]
F value	7.045	7.425	4.045	1.181	9.447	17.558
P value	0.000	0.000	0.008	0.347	0.000	0.000

Data are presented as mean ± standard deviation. EDV: end-diastolic velocity; ESV: end-systolic velocity; RI: resistance index. [*]$P < 0.05$ vs. left middle cerebral artery; [§]$P < 0.05$ vs. sham operation group at 24 h; [a]$P < 0.05$ vs. HI group at 0 h; [b]$P < 0.05$ vs. HI group at 4 h; [c]$P < 0.05$ vs. HI group at 8 h; [d]$P < 0.05$ vs. HI group at 12 h.
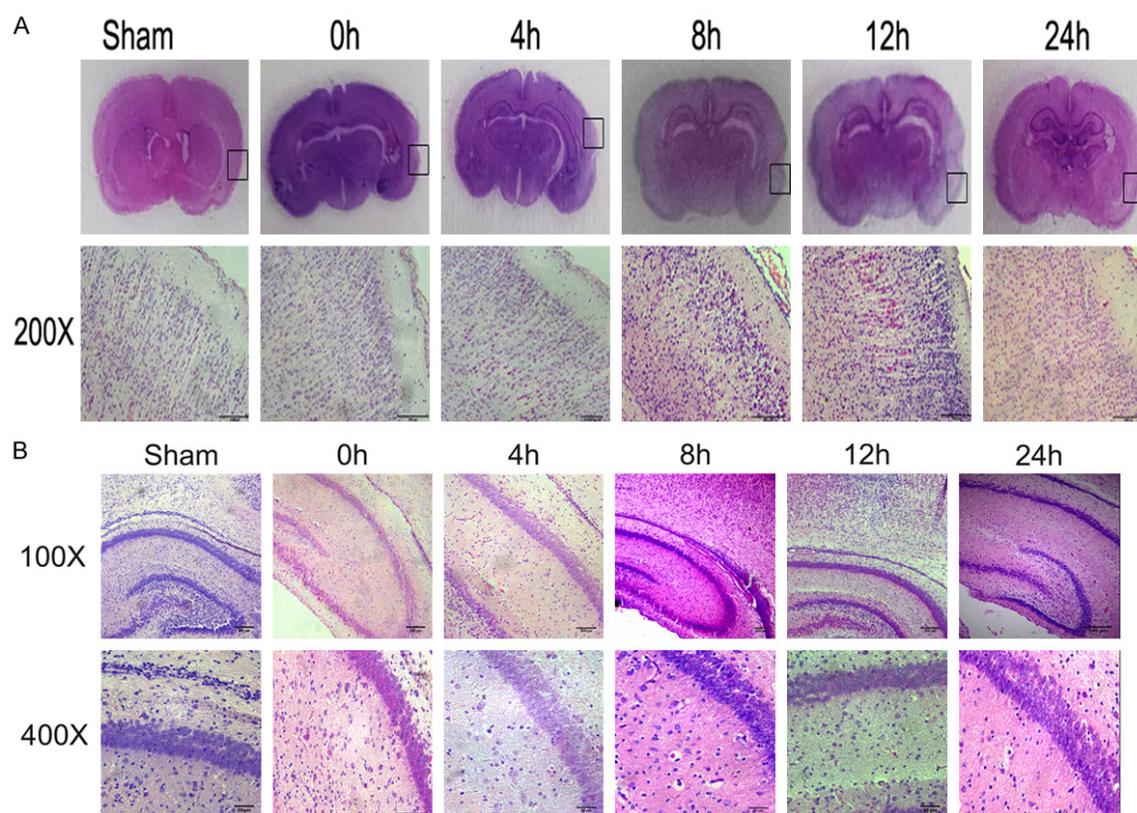
Figure 3. Histopathology of hippocampal and cerebral cortex brain tissue at various times after surgery/hypoxia. (A) Brain coronal sections from sham control animals and animals after hypoxia-ischemia were stained with hematoxylin-eosin (H&E). Lower panel represents magnification (200×) of the ipsilateral hemisphere area (marked with rectangles in A). Note the loss of neurons, signs of cerebral edema, and typical red neurons in the cortex of ipsilateral hemisphere at 8 h and 12 h, and these phenomena were slightly alleviated in 24 h. (B) Representative sections of the pyramidal cell layer of the right hippocampus. The HI group (0 h, 4 h, 8 h, 12 h, and 24 h) exhibited the development of features characteristic of acute ischemia, including a decrease in cell density, the appearance of cellular vacuoles, and nuclear pyknosis and fragmentation. Photomicrographs are representative of observations made from eight animals per group.

ing proteins (**Figure 6**). Compared with the sham operation group, the HI group had elevat-

ed mRNA expression of NLRP3 at 4 h, 8 h, and 24 h, enhanced mRNA expression of caspase-1
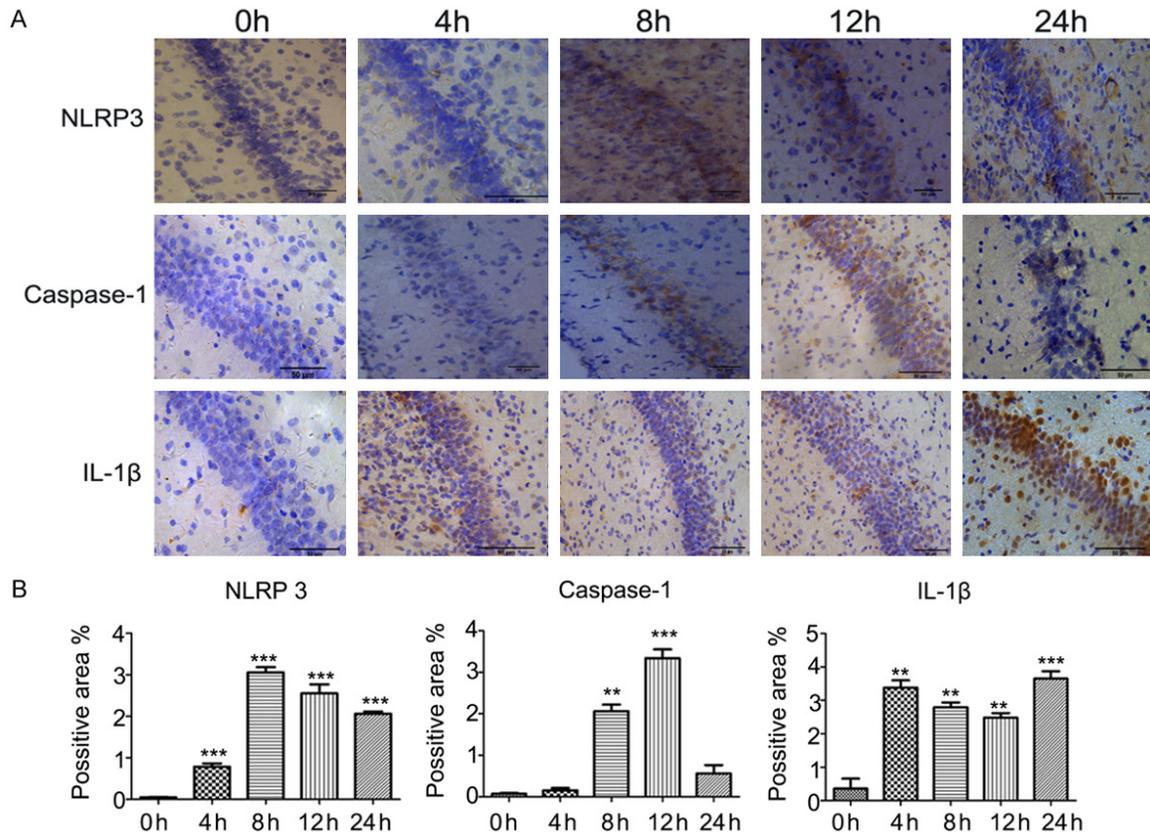
Figure 4. Expression of NLRP3, caspase-1, and IL-1β proteins in brain tissue evaluated by immunohistochemistry. A. Representative images showing sections of brain tissue from the HI group stained using immunohistochemistry techniques. The expression levels of NLRP3, caspase-1, and IL-1β proteins were determined at 0 h, 4 h, 8 h, 12 h, and 24 h after surgery/hypoxia. B. Averaged semi-quantitative data comparing the expression levels of NLRP3, caspase-1, and IL-1β proteins between the various time points. $**P < 0.01$, $***P < 0.001$ vs. 0 h.

at 12 h and 24 h, and increased mRNA expression of IL1-β at 8 h, 12 h, and 24 h ($P < 0.05$ for all).

Discussion

Notable findings of the present study were that increased mRNA and protein expressions of NLRP3, caspase-1, and IL-1β were observed within 4-8 h in a rat model of HI brain injury.

These observations provide a basis for the start time for early diagnosis and treatment of hypoxic-ischemic brain damage. Furthermore, our research raises the possibility that NLRP3/caspase-1/IL-1β signaling may be a target for novel neuroprotective therapies in the setting of neonatal HI brain injury.

Clinical trials have proven that it is effective to start hypothermia treatment within 3-6 hours, and at present, therapeutic hypothermia is

the standard treatment for hypoxic-ischemic encephalopathy (HIE) [23, 24]. However, the rate of death or disability in hypothermia treatment ranged from 44-55% in the clinical trials [25]. Thus, it is very important to optimize current hypothermia protocols. Early identification of non-responders to treatment will improve the outcome. This is not possible yet, as specific biomarkers and the changing rules of these biomarkers are still unfounded. The pathophysiologic process of HIE is not static, but constantly evolving. The choice of intervention window is very important for the prognosis of HIE.

Inflammation is considered to be an important pathophysiologic factor of cerebral ischemic injury. Perinatal infection is a risk factor for disability and death of full-term newborns. Recent studies have shown that the neonatal infection rate of asphyxiated newborns is significantly higher than that of the general population [26]. The NLRP3 inflammasome is an important part
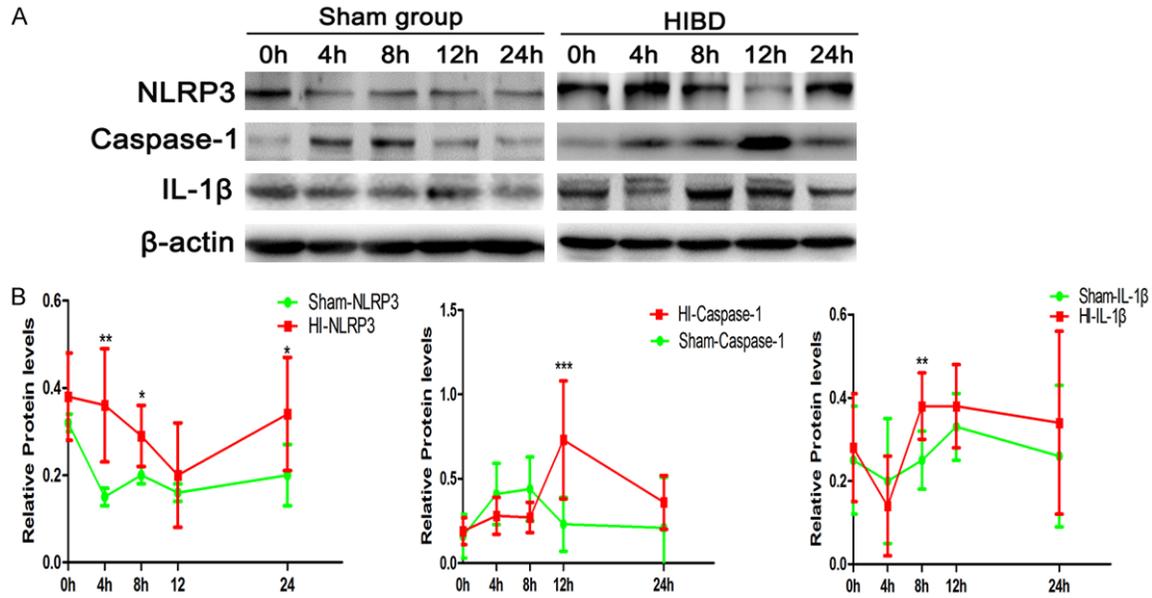
Figure 5. Expression of NLRP3, caspase-1, and IL-1β proteins in brain tissue evaluated by western blot. A. Representative immunoblots illustrating the expressions levels of NLRP3, caspase-1, and IL-1β proteins in brain tissue from the HI and sham operation groups at varying times (0 h, 4 h, 8 h, 12 h and 24 h) after surgery/hypoxia. B. Averaged semi-quantitative data comparing the expression levels of NLRP3, caspase-1, and IL-1β proteins between the HI and sham operation groups. *$P < 0.05$, **$P < 0.01$, ***$P < 0.001$ vs. sham operation group.
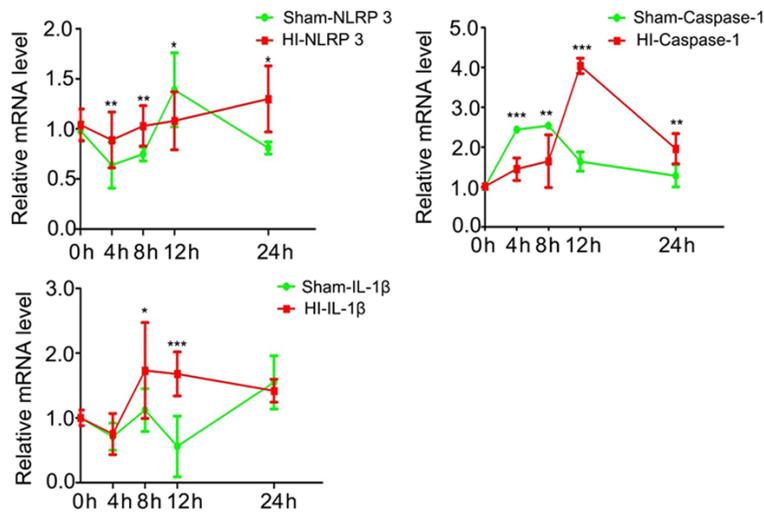
Figure 6. Expression of NLRP3, caspase-1, and IL-1β mRNA in brain tissue evaluated by RT-PCR. Averaged semi-quantitative data are shown comparing the expression levels of NLRP3, caspase-1, and IL-1β mRNA in brain tissue between the HI and sham operation groups at varying times (0 h, 4 h, 8 h, 12 h and 24 h) after surgery/hypoxia. *$P < 0.05$, **$P < 0.01$, ***$P < 0.001$ vs. sham operation group.

observe its early changes after hypoxia-ischemia brain injury. Neurons that express receptors for cytokines such as IL-1β and IL-18 and are particularly sensitive to these cytokines [27, 28]. Stimuli of pyroptosis include pathogen-associated molecular patterns and damage-associated molecular patterns, and these factors are primarily recognized by NLRs such as the NLRP3 inflammasome [29, 30], which recruits caspase-1 to increase the levels of IL-1β and IL-18 and thereby stimulate an inflammatory response and cellular toxicity. Recent research has indicated that activation of the NLRP3 inflammasome also occurs in neonatal rats after HI brain injury. For example, microglia exhibited upregulated expression of IL-1β and NLRP3 inflammasome-associated genes 24 h after inflammation-sensitized HI brain injury in 7-day-old neonatal rats [31], while 10-day-old neonatal rats were observed to have increased

of the innate immune system, which can mediate the activation of caspase-1 and the secretion of proinflammatory cytokines IL-1β/IL-18. The innate immune system is the first line of host defense, so we chose to study NLRP3 to

expressions of caspase-1 and IL-1β at 24 h after HI brain injury [16]. Furthermore, microglial activation was detected as early as 2 h after HI in rat models, suggesting that activated microglia may play a central role in triggering neuroinflammation and damage to the immature brain [18]. Therefore, we evaluated NLRP3 inflammasome signaling at 5 time points during the first 24 h after HI injury. An important finding of this study was that the HI group showed significantly increased levels of NLRP3 mRNA (RT-PCR) and protein (immunohistochemistry and western blot) at 4 h. Furthermore, caspase-1 and IL-1β expression levels were also elevated at 8-12 h, illustrating that activation of NLRP3 inflammasome-related signaling occurred within 4 h of neonatal HI brain injury.

In the present study, the elevated levels of NLRP3 protein and mRNA expression were well-maintained between 4 h and 24 h. A similar phenomenon was observed for IL-1β between 8 h and 24 h. Notably, caspase-1 expression in the HI group showed an initial elevation, particularly at 12 h, but this was followed by a subsequent decline at 24 h. Temporal changes in caspase-1 expression vary between different nervous system diseases [32-35]. We speculate that the upregulation of caspase-1 protein in the HI group at 12 h followed by a decrease at 24 h, is related to different stages in the pathogenesis of HI encephalopathy [36, 37]. In the first stage, primary cell injury occurs because reduced cerebral blood flow and oxygen transport initiate a harmful biochemical cascade that leads to cytotoxicity, edema and apoptosis. This would result in activation of NLRP3 signaling and caspase-1, whose expression level would peak after a time lag. During the next stage, resuscitation improves cerebral oxygenation and perfusion, leading to rapid partial or complete recovery of intracellular phosphocreatine and ATP levels. This, in turn, may lead to a subsequent decline in caspase-1, as observed in our study at 24 h. Thus, it would be interesting to establish whether a secondary increase in caspase-1 expression occurred after 24 h in rat model of neonatal HI brain injury.

The present study developed a model of HI brain injury in 7-day-old neonatal rats, which are thought to have a level of brain maturity similar to that of fetuses at 36-40 weeks of gestation [38, 39]. Histopathologic analysis at 24 h demonstrated changes that were characteristic of HI brain injury. Unlike most previous studies, we also used craniocerebral ultrasound to evaluate the success of our model. Notably, we observed that the HI group showed diffuse heterogenous enhancement of the brain parenchyma at 24 h, and some of the animals also exhibited the phenomenon of vertebrobasilar artery stealing with opposite directionality of blood flow for the vertebral artery and ipsilateral common carotid artery. The phenomenon of vertebrobasilar stealing has been described in adults [40], but reports in neonates are rare. Thus, we believe that brain ultrasound may be instructive in neonates with HI brain injury.

Elevated mRNA and protein expressions of NLRP3, caspase-1, and IL-1β were observed within 4-8 h of HI brain injury in the neonatal rat. These findings suggest that the treatment of HIE should be earlier than 4 hours, and if possible, sooner. In addition, the NLRP3/caspase-1/IL-1β signaling pathway might be a novel therapeutic target for the development of strategies to treat neonatal HI brain injury.

Acknowledgements

Disclosure of conflict of interest

None.

Address correspondence to: Chunying Liu, College of Integrated Traditional Chinese and Western Medicine, Liaoning University of Traditional Chinese Medicine, Shenyang, China. E-mail: chunying1951@163.com

References

[1] Tagin M, Abdel-Hady H, ur Rahman S, Azzopardi DV and Gunn AJ. Neuroprotection for perinatal hypoxic ischemic encephalopathy in low- and middle-income countries. J Pediatr 2015; 167: 25-28.

[2] Arnaez J, García-Alix A, Arca G, Caserío S, Valverde E, Moral MT, Benavente-Fernández I and Lubián-López S. Population-based study of the national implementation of therapeutic hypothermia in infants with hypoxic-ischemic encephalopathy. Ther Hypothermia Temp Manag 2018; 8: 24-29.

[3] Conway JM, Walsh BH, Boylan GB and Murray DM. Mild hypoxic ischaemic encephalopathy and long term neurodevelopmental outcome - A systematic review. Early Hum Dev 2018; 120: 80-87.

[4] Rodríguez M, Valez V, Cimarra C, Blasina F and Radi R. Hypoxic-ischemic encephalopathy and mitochondrial dysfunction: facts, unknowns, and challenges. Antioxid Redox Signal 2020; 33: 247-262.

[5] Laptook AR, Shankaran S, Tyson JE, Munoz B, Bell EF, Goldberg RN, Parikh NA, Ambalavanan N, Pedroza C, Pappas A, Das A, Chaudhary AS, Ehrenkranz RA, Hensman AM, Van Meurs KP, Chalak LF, Khan AM, Hamrick SEG, Sokol GM, Walsh MC, Poindexter BB, Faix RG, Watterberg KL, Frantz ID 3rd, Guillet R, Devaskar U, Truog WE, Chock VY, Wyckoff MH, McGowan EC, Carlton DP, Harmon HM, Brumbaugh JE, Cotten CM, Sánchez PJ, Hibbs AM and Higgins RD. Effect of therapeutic hypothermia initiated after 6 hours of age on death or disability among newborns with hypoxic-ischemic encephalopathy: a randomized clinical trial. JAMA 2017; 318: 1550-1560.

[6] Shankaran S, Laptook AR, Pappas A, McDonald SA, Das A, Tyson JE, Poindexter BB, Schibler K, Bell EF, Heyne RJ, Pedroza C, Bara R, Van Meurs KP, Huitema CMP, Grisby C, Devaskar U, Ehrenkranz RA, Harmon HM, Chalak LF, DeMauro SB, Garg M, Hartley-McAndrew ME, Khan AM, Walsh MC, Ambalavanan N, Brumbaugh JE, Watterberg KL, Shepherd EG, Hamrick SEG, Barks J, Cotten CM, Kilbride HW and Higgins RD. Effect of depth and duration of cooling on death or disability at age 18 months among neonates with hypoxic-ischemic encephalopathy: a randomized clinical trial. JAMA 2017; 318: 57-67.

[7] Jacobs SE, Morley CJ, Inder TE, Stewart MJ, Smith KR, McNamara PJ, Wright IM, Kirpalani HM, Darlow BA and Doyle LW. Whole-body hypothermia for term and near-term newborns with hypoxic-ischemic encephalopathy: a randomized controlled trial. Arch Pediatr Adolesc Med 2011; 165: 692-700.

[8] Lv HY, Wu SJ, Wang QL, Yang LH, Ren PS, Qiao BJ, Wang ZY, Li JH, Gu XL and Li LX. Effect of erythropoietin combined with hypothermia on serum tau protein levels and neurodevelopmental outcome in neonates with hypoxic-ischemic encephalopathy. Neural Regen Res 2017; 12: 1655-1663.

[9] Youn YA, Kim JH, Yum SK, Moon CJ, Lee IG and Sung IK. The hospital outcomes compared between the early and late hypothermia-treated groups in neonates. J Matern Fetal Neonatal Med 2016; 29: 2288-2292.

[10] Higgins RD, Raju T, Edwards AD, Azzopardi DV, Bose CL, Clark RH, Ferriero DM, Guillet R, Gunn AJ, Hagberg H, Hirtz D, Inder TE, Jacobs SE, Jenkins D, Juul S, Laptook AR, Lucey JF, Maze M, Palmer C, Papile L, Pfister RH, Robertson NJ, Rutherford M, Shankaran S, Silverstein FS, Soll RF, Thoresen M and Walsh WF; Eunice Kennedy Shriver National Institute of Child Health and Human Development Hypothermia Workshop Speakers and Moderators. Hypothermia and other treatment options for neonatal encephalopathy: an executive summary of the Eunice Kennedy Shriver NICHD workshop. J Pediatr 2011; 159: 851-858, e851.

[11] Yang Y, Wang H, Kouadir M, Song H and Shi F. Recent advances in the mechanisms of NLRP3 inflammasome activation and its inhibitors. Cell Death Dis 2019; 10: 128.

[12] Aridas JD, Yawno T, Sutherland AE, Nitsos I, Ditchfield M, Wong FY, Fahey MC, Malhotra A, Wallace EM, Jenkin G and Miller SL. Detecting brain injury in neonatal hypoxic ischemic encephalopathy: closing the gap between experimental and clinical research. Exp Neurol 2014; 261: 281-290.

[13] Paramel Varghese G, Folkersen L, Strawbridge RJ, Halvorsen B, Yndestad A, Ranheim T, Krohg-Sørensen K, Skjelland M, Espevik T, Aukrust P, Lengquist M, Hedin U, Jansson JH, Fransén K, Hansson GK, Eriksson P and Sirsjö A. NLRP3 inflammasome expression and activation in human atherosclerosis. J Am Heart Assoc 2016; 5: e003031.

[14] Saresella M, La Rosa F, Piancone F, Zoppis M, Marventano I, Calabrese E, Rainone V, Nemni R, Mancuso R and Clerici M. The NLRP3 and NLRP1 inflammasomes are activated in Alzheimer's disease. Mol Neurodegener 2016; 11: 23.

[15] Wu C, Zhang G, Chen L, Kim S, Yu J, Hu G, Chen J, Huang Y, Zheng G and Huang S. The role of NLRP3 and IL-1β in refractory epilepsy brain injury. Front Neurol 2019; 10: 1418.

[16] Serdar M, Kempe K, Rizazad M, Herz J, Bendix I, Felderhoff-Muser U and Sabir H. Early pro-inflammatory microglia activation after inflammation-sensitized hypoxic-ischemic brain injury in neonatal rats. Front Cell Neurosci 2019; 13: 237.

[17] Chen A, Xu Y and Yuan J. Ginkgolide B ameliorates NLRP3 inflammasome activation after hypoxic-ischemic brain injury in the neonatal male rat. Int J Dev Neurosci 2018; 69: 106-111.

[18] Chen D, Dixon BJ, Doycheva DM, Li B, Zhang Y, Hu Q, He Y, Guo Z, Nowrangi D, Flores J, Filippov V, Zhang JH and Tang J. IRE1alpha inhibition decreased TXNIP/NLRP3 inflammasome activation through miR-17-5p after neonatal hypoxic-ischemic brain injury in rats. J Neuroinflammation 2018; 15: 32.

[19] Rice JE 3rd, Vannucci RC and Brierley JB. The influence of immaturity on hypoxic-ischemic brain damage in the rat. Ann Neurol 1981; 9: 131-141.

[20] Huang L, Zhao F, Qu Y, Zhang L, Wang Y and Mu D. Animal models of hypoxic-ischemic encephalopathy: optimal choices for the best outcomes. Rev Neurosci 2017; 28: 31-43.

[21] Belayev L, Alonso OF, Busto R, Zhao W and Ginsberg MD. Middle cerebral artery occlusion in the rat by intraluminal suture. Neurological and pathological evaluation of an improved model. Stroke 1996; 27: 1616-1622; discussion 1623.

[22] Zhu ZH, Peng KP, Liu MH and Tian GX. Acoustic radiation force impulse imaging with virtual touch tissue quantification enables characterization of mild hypoxic-ischemic brain damage in neonatal rats. J Ultrasound Med 2019; 38: 1797-1805.

[23] Thoresen M, Tooley J, Liu X, Jary S, Fleming P, Luyt K, Jain A, Cairns P, Harding D and Sabir H. Time is brain: starting therapeutic hypothermia within three hours after birth improves motor outcome in asphyxiated newborns. Neonatology 2013; 104: 228-233.

[24] Silveira RC and Procianoy RS. Hypothermia therapy for newborns with hypoxic ischemic encephalopathy. J Pediatr (Rio J) 2015; 91: S78-83.

[25] Nannan NN, Groenewald P, Pillay-van Wyk V, Nicol E, Msemburi W, Dorrington RE and Bradshaw D. Child mortality trends and causes of death in South Africa, 1997 - 2012, and the importance of a national burden of disease study. S Afr Med J 2019; 109: 480-485.

[26] Jacobs SE, Berg M, Hunt R, Tarnow-Mordi WO, Inder TE and Davis PG. Cooling for newborns with hypoxic ischaemic encephalopathy. Cochrane Database Syst Rev 2013; 2013: Cd003311.

[27] Fogal B and Hewett SJ. Interleukin-1beta: a bridge between inflammation and excitotoxicity? J Neurochem 2008; 106: 1-23.

[28] Zhang J, Wu C, Gao L, Du G and Qin X. Astragaloside IV derived from Astragalus membranaceus: a research review on the pharmacological effects. Adv Pharmacol 2020; 87: 89-112.

[29] Felderhoff-Mueser U, Schmidt OI, Oberholzer A, Buhrer C and Stahel PF. IL-18: a key player in neuroinflammation and neurodegeneration? Trends Neurosci 2005; 28: 487-493.

[30] Palm NW and Medzhitov R. Role of the inflammasome in defense against venoms. Proc Natl Acad Sci U S A 2013; 110: 1809-1814.

[31] Strowig T, Henao-Mejia J, Elinav E and Flavell R. Inflammasomes in health and disease. Nature 2012; 481: 278-286.

[32] Benchoua A, Guegan C, Couriaud C, Hosseini H, Sampaio N, Morin D and Onteniente B. Specific caspase pathways are activated in the two stages of cerebral infarction. J Neurosci 2001; 21: 7127-7134.

[33] Chen CY, Sun WZ, Kang KH, Chou HC, Tsao PN, Hsieh WS and Fu WM. Hypoxic preconditioning suppresses glial activation and neuroinflammation in neonatal brain insults. Mediators Inflamm 2015; 2015: 632592.

[34] de Rivero Vaccari JP, Lotocki G, Marcillo AE, Dietrich WD and Keane RW. A molecular platform in neurons regulates inflammation after spinal cord injury. J Neurosci 2008; 28: 3404-3414.

[35] Hara H, Friedlander RM, Gagliardini V, Ayata C, Fink K, Huang Z, Shimizu-Sasamata M, Yuan J and Moskowitz MA. Inhibition of interleukin 1beta converting enzyme family proteases reduces ischemic and excitotoxic neuronal damage. Proc Natl Acad Sci U S A 1997; 94: 2007-2012.

[36] Greco P, Nencini G, Piva I, Scioscia M, Volta CA, Spadaro S, Neri M, Bonaccorsi G, Greco F, Cocco I, Sorrentino F, D'Antonio F and Nappi L. Pathophysiology of hypoxic-ischemic encephalopathy: a review of the past and a view on the future. Acta Neurol Belg 2020; 120: 277-288.

[37] Nuñez A, Benavente I, Blanco D, Boix H, Cabañas F, Chaffanel M, Fernández-Colomer B, Fernández-Lorenzo JR, Loureiro B, Moral MT, Pavón A, Tofé I, Valverde E and Vento M. [Oxidative stress in perinatal asphyxia and hypoxic-ischaemic encephalopathy]. An Pediatr (Barc) 2018; 88: 228.e221-228.e229.

[38] Goren B, Cakir A, Ocalan B, Serter Kocoglu S, Alkan T, Cansev M and Kahveci N. Long-term cognitive effects of uridine treatment in a neonatal rat model of hypoxic-ischemic encephalopathy. Brain Res 2017; 1659: 81-87.

[39] Rumajogee P, Bregman T, Miller SP, Yager JY and Fehlings MG. Rodent hypoxia-ischemia models for cerebral palsy research: a systematic review. Front Neurol 2016; 7: 57.

[40] Konda S, Dayawansa S, Singel S and Huang JH. Pseudo subclavian steal syndrome: case report. Int J Surg Case Rep 2015; 16: 177-180.